

Instability of a Möbius Strip Minimal Surface and a Link with Systolic Geometry

Adriana I. Pesci,¹ Raymond E. Goldstein,¹ Gareth P. Alexander,² and H. Keith Moffatt¹

¹*Department of Applied Mathematics and Theoretical Physics, Centre for Mathematical Sciences,
University of Cambridge, Wilberforce Road, Cambridge CB3 0WA, United Kingdom*

²*Department of Physics and Centre for Complexity Science, University of Warwick, Coventry CV4 7AL, United Kingdom*

(Received 1 December 2014; published 24 March 2015)

We describe the first analytically tractable example of an instability of a nonorientable minimal surface under parametric variation of its boundary. A one-parameter family of incomplete Meeks Möbius surfaces is defined and shown to exhibit an instability threshold as the bounding curve is opened up from a double-covering of the circle. Numerical and analytical methods are used to determine the instability threshold by solution of the Jacobi equation on the double covering of the surface. The unstable eigenmode shows excellent qualitative agreement with that found experimentally for a closely related surface. A connection is proposed between systolic geometry and the instability by showing that the shortest noncontractible closed geodesic on the surface (the systolic curve) passes near the maximum of the unstable eigenmode.

DOI: 10.1103/PhysRevLett.114.127801

PACS numbers: 68.15.+e, 02.40.-k, 47.20.Ky, 83.10.-y

The subject of this Letter lies at the intersection of several branches of physics and mathematics: minimal surfaces, soap films, topological transitions, computation, and shortest closed noncontractible geodesics on surfaces, known as systolic curves [1]. Euler's discovery in 1744 [2] of the catenoid as the area-minimizing surface spanning two circular loops effectively began the study of minimal surfaces, which are now known to play a role in areas as diverse as soap films [3], supramolecular assemblies [4], defect structures [5], as well as general relativity [6], string theory [7], and even architecture [8].

Of particular interest for centuries has been not only the issue of determining a minimal surface supported by a given “frame,” but also the competition between different possible surfaces on the same frame [9]. Thus, in the case of two parallel circular rings whose separation H is varied, the catenoid solution ceases to be the minimum energy state beyond a calculable value H^* , and ceases to exist at all beyond a critical value H_c ($> H^*$). For $H^* < H < H_c$, the lower energy state is the Goldschmidt solution [10], discs spanning each loop, connected by a singular line segment. In laboratory realizations of this setup with soap films, slow variation of the spacing beyond H_c triggers collapse of the catenoid with a complex set of neck-pinching singularities [11,12], leading dynamically to the Goldschmidt solution (minus the unphysical connection). Dynamics akin to the Rayleigh-Plateau instability occur not only in capillary phenomena, but even in exotic contexts such as the instability of black strings [13].

The catenoid is important in the study of minimal surfaces because its high degree of symmetry and simplicity make it possible to determine, in detail, the nature of its linear instability at H_c from the second variation of the area functional [14]. The unstable eigenfunction at the instability point is the solution of the Jacobi equation $(\nabla^2 - 2K)u = 0$,

where K is the Gaussian curvature. Axisymmetry of the catenoid reduces the Jacobi equation to a one-dimensional Schrödinger equation with a sech-squared potential. This approach has been extended to transitions between the helicoid and the catenoid [15], locally isometric surfaces that interconvert without a singularity.

Recent work has indicated that, when the frame supporting a soap film is deformed so as to render it unstable, the location and character of the ensuing singularity that marks the topological transition depend on the topology of the initial minimal surface. For example, the catenoid instability leads to a singularity in the bulk of the film, whereas a Möbius strip minimal surface transforms to a disc through a boundary singularity [16–18]. Moreover, at least in these two cases, we observed that the location of the singularity (bulk or boundary) can be determined by studying the topology of the systolic curve on the surface [1,19]. Historically, there has been great interest in such curves [20], but apart from quantum error correction [21], it appears that there have been no applications of systolic geometry in physics.

Given that the prototype models for topological transitions of a bounded film are the catenoid (for bulk singularities) and the Möbius strip (for boundary singularities), it is natural to seek an analytically tractable example of an instability for a nonorientable surface. Here, we present one, using the surface known as a Meeks Möbius strip [22]. This is a complete surface [23] with total curvature (the surface integral of K) of -6π . As is well known, the only stable complete minimal surfaces in \mathbb{R}^3 are planes [24,25]. One, therefore, deduces that it is impossible to continue any bounded nonplanar minimal surface to its complete form without it becoming unstable at a finite size. One of our primary results is the identification, for the Meeks surface, of a one-parameter family of contours defining a sequence of bounded surfaces which, like the catenoid, are stable

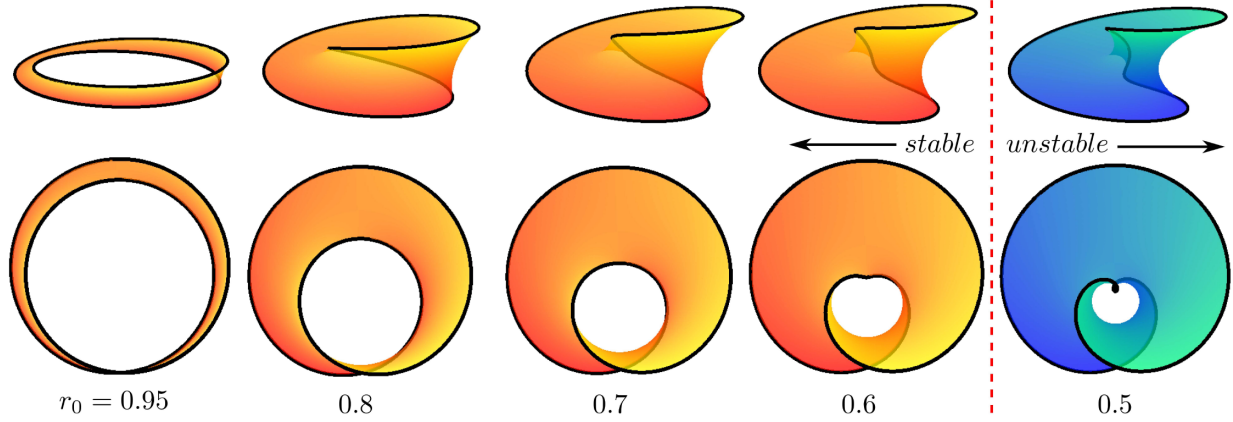


FIG. 1 (color online). Incomplete Meeks Möbius minimal surfaces. Two views are shown for each choice of the parameter r_0 . Surfaces for $r_0 \lesssim 0.54$ are linearly unstable.

below a threshold parameter value and unstable above. We deduce the point of instability through a combination of straightforward analytical approximations and numerical studies of the Jacobi equation. In a further connection between systolic geometry and stability theory, we show that the systolic curve on the unstable minimal surface approaches the maximum of the unstable eigenfunction, confirming one's intuition that the instability begins at the narrowest part of the neck.

The Meeks Möbius surface [22] is most compactly given by its Weierstrass-Enneper representation I [23] in terms of a holomorphic function $f(\zeta) = i(\zeta - 1)^2/\zeta^4$ and a meromorphic function $g(\zeta) = \zeta^2(\zeta + 1)/(\zeta - 1)$, with fg^2 holomorphic. These functions provide the components of the vector $\Phi = [f(1 - g^2), if(1 + g^2), 2fg]$ which, with $\zeta = u + iv$, determines the surface $\mathbf{X}(u, v) = \Re[\int d\zeta' \Phi]$, where $\mathbf{X}(u, v) = (x, y, z)$ are the Cartesian coordinates. This representation guarantees that the mean curvature vanishes and that the parametrization (u, v) corresponds to “isothermal” coordinates. Indeed, the metric is $ds^2 = W(du^2 + dv^2)$, where $W = |f|^2(1 + |g|^2)^2$, and the Gaussian curvature is $K = -4|g'|^2|f|^{-2}(1 + |g|^2)^{-4}$.

If we write $u = r \cos \theta$, $v = r \sin \theta$, then the surface takes on a particularly simple form

$$x = -\alpha \sin \theta - \beta \sin 2\theta - \gamma \sin 3\theta, \quad (1)$$

$$y = \alpha \cos \theta + \beta \cos 2\theta + \gamma \cos 3\theta, \quad (2)$$

$$z = -2\alpha \sin \theta, \quad (3)$$

where $\alpha = r - r^{-1}$, $\beta = r^2 + r^{-2}$, $\gamma = (1/3)(r^3 - r^{-3})$. Alternatively, if $r = e^p$, $\alpha = 2 \sinh p$, $\beta = 2 \cosh(2p)$, and $\gamma = (2/3) \sinh(3p)$. The complete surface is traced out as a double-covering for $0 \leq r \leq \infty$ ($-\infty \leq p \leq \infty$) and $0 \leq \theta \leq 2\pi$. These representations make clear, immediately, the fundamental symmetry of the surface: $\mathbf{X}(r, \theta) = -\mathbf{X}(1/r, \theta + \pi)$ or $\mathbf{X}(p, \theta) = -\mathbf{X}(-p, \theta + \pi)$. While the

(r, θ) parametrization is more intuitive, with r a radial coordinate, the (p, θ) choice is often more convenient for algebraic and computational purposes.

When the parameter r (or p) is restricted to a finite interval whose endpoints are consistent with the symmetry of the surface, i.e., $r_0 \leq r \leq 1/r_0$, the resulting surface is a Möbius strip with boundary $(x(r_0, \theta), y(r_0, \theta), z(r_0, \theta))$. Figure 1 shows the progression of surface shapes as r_0 is decreased from unity. Since the surface given by $r_0 \rightarrow 1$ is clearly stable, while that for $r_0 \rightarrow 0$ is unstable, there must exist a finite critical value that determines the onset of the instability. That critical point can be determined by finding the value of r_0 for which the second variation of the area functional vanishes. This is equivalent to seeking a displacement field $\psi(u, v)$ normal to the surface which vanishes on the boundary and is a solution of the Jacobi equation, $(\nabla^2 - 2KW)\psi = \lambda W\psi$, for the particular case $\lambda = 0$, where now $\nabla^2 = \partial_{uu} + \partial_{vv}$. For a physical soap film of thickness h , $\lambda = -\rho h \omega^2 / \sigma$, where ρ is the film density, σ is the surface tension, and ω is the oscillation frequency [15]. The condition $\lambda = 0$, thus, marks the boundary between oscillatory behavior and instability. In the variables (p, θ) , the Jacobi equation is

$$\psi_{pp} + \psi_{\theta\theta} + 4 \frac{\cosh 2p + 2 \sinh p \cos \theta + 2 \sin^2 \theta}{(\cosh p \cosh 2p - \sinh 2p \cos \theta)^2} \psi = 0. \quad (4)$$

Because we are dealing with a nonorientable surface, we use an orientable double covering, for which it is possible to find a global normal vector field. In this double covering, the normal vector satisfies $\hat{\mathbf{n}}(p, \theta) = -\hat{\mathbf{n}}(-p, \theta + \pi)$ [equivalently $\hat{\mathbf{n}}(r, \theta) = -\hat{\mathbf{n}}(1/r, \theta + \pi)$]. Thus, in order to obtain a physically meaningful displacement vector field $\psi \hat{\mathbf{n}}$, we require $\psi(p, \theta) = -\psi(-p, \theta + \pi)$ [equivalently $\psi(r, \theta) = -\psi(1/r, \theta + \pi)$].

First, we discuss the numerical solution of Eq. (4), and the determination of the critical value p_c and the

unstable eigenfunction ψ_c . Because of the antisymmetry discussed above, it is only necessary to solve the problem for $0 \leq \theta \leq \pi$, with the boundary condition $\psi(p, 0) = -\psi(-p, \pi)$, along with the Dirichlet boundary condition at the bounding curve, $\psi(\pm p_c, \theta) = 0$. These boundary conditions can readily be accommodated within a standard finite-difference scheme on a regular grid in both θ and p . If, however, one uses the more physical parameter r , then a hyperbolic grid $r(m) = r_0^{2m/M-1}$ for $m = 1, 2, \dots, M$ allows easy implementation of the boundary conditions. We determined the instability threshold by finding, for a coarse grid spacing, the value of p for which there first appears a zero eigenvalue of the matrix corresponding to the finite-difference discretization of Eq. (4). Refinement of the grid was used to sharpen this numerical estimate to $p_c \approx -0.607$ ($r_c \approx 0.545$).

Figures 2(a) and 2(b) show, for $p = p_c$ and on the double covering, the quantities KW , which enters the Jacobi equation (4), and the numerically obtained critical mode ψ_c . The maximum amplitude of the Gaussian curvature term is anticorrelated with the maxima of the modes. The latter [Fig. 2(b)] are located approximately at the center of each covering [Fig. 2(b)]. Because the Jacobi equation describes the oscillations of a curved soap film, and the Gaussian curvature term is small in the interior of the domain, the mode shape approximates that of a flat film clamped at its edges. This lowest eigenfunction has the minimum possible number of nodes. Figure 2(c) shows the critical Meeks surface ($p = p_c$) color coded by the amplitude of ψ_c . The maximum amplitude occurs in the “throat” of the surface, which is locally similar in shape to a catenoid, and directly opposite the nodal line in ψ_c at $\theta = \pi$. This nodal line coincides with the line of symmetry of the surface, which is the unique straight line on it. The arrows in Fig. 2(c) represent the vectorial displacement field $\psi_c \hat{\mathbf{n}}$ along the systolic curve (discussed below). The pattern of displacements shown is qualitatively identical to that observed in experiment [16,18], where the interface collapses towards the frame.

From the results in Fig. 2, we see that the critical mode ψ_c has a large amplitude in regions where the Gaussian curvature term $-2KW$ is small, and the Dirichlet condition

$\psi_c = 0$ on the surface boundary dominates the locally large value of the Gaussian curvature there. Therefore, the presence of K makes only a minor change to the shape of the unstable mode. This lack of correlation between KW and ψ suggests that an approximate analytical approach to solving the Jacobi equation is to reduce it to a one-dimensional equation by averaging over the periodic variable θ . This integration yields the approximate Jacobi equation $\bar{\psi}_{pp} - 2\overline{KW}\bar{\psi} \approx 0$. The average \overline{KW} is a complicated combination of hyperbolic functions that, remarkably, can be represented with great accuracy ($\sim 1\%$) by a sum of sech-squared terms,

$$\bar{\psi}_{pp} + U_0 \{ \text{sech}^2[\alpha(p-a)] + \text{sech}^2[\alpha(p+a)] \} \bar{\psi} = 0, \quad (5)$$

where $a = 0.4456$, $\alpha a = \tanh^{-1}(\sqrt{5/7})$, and $U_0 = \alpha^2$. Thus, integration over the angular variables for both the catenoid and the Meeks surfaces yields one-dimensional Schrödinger equations, the former having a sech-squared potential, and the latter with one of the variants of the Morse-Rosen double-well potential [26] introduced by Stec [27]. Through the change of variables $q = \tanh \alpha p$, Eq. (5) reduces to a Heun equation [28]. Rather than dealing with a global solution of that equation, we focus only on the region far from the double-well minima

$$(1 - q^2)\psi_{qq} - 2q\psi_q + \frac{1 + \kappa^2}{1 - \kappa^2}\psi = 0, \quad (6)$$

where $\kappa^2 = \tanh^2(\alpha a) = 5/7$. Thus, $(1 + \kappa^2)/(1 - \kappa^2) = n(n+1)$ for $n = 2$. This has the solution $\psi = Q_2(p) = (\alpha p/2)[3 \tanh^2(\alpha p) - 1] - (3/2) \tanh(\alpha p)$, the Legendre function of the second kind. The requirement that $\psi = 0$ on the boundary is satisfied by $p^* = \pm 0.6178\dots$ such that $Q_2(p^*) = 0$, which yields $r_0 \approx 0.539$, within 1% of the numerical result.

When the condition $\overline{KW}\bar{\psi} \approx \overline{KW}\bar{\psi}$ is satisfied, the resulting one-dimensional equation (5) is a Schrödinger equation for a bounded double-well potential. A characteristic of this potential is that for energies close to zero (i.e., energies close to those of free particle states) approximating

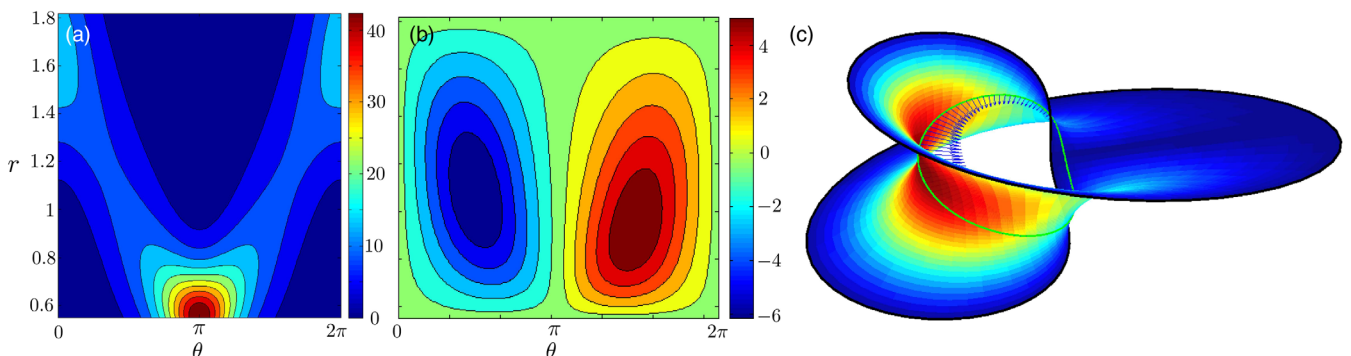


FIG. 2 (color online). The critical surface. (a) The term $-2KW$ in the (r, θ) plane for $r_0 = 0.545$. (b) Unstable eigenfunction ψ_c on the double covering. (c) Critical surface, color coded by the magnitude of ψ_c .

the double well potential by two delta functions of appropriate amplitude and located at the position of the minima yields a surprisingly good first approximation to the wave function. For the Meeks Möbius surface, the potential is replaced by $U_0[\delta(p+a) + \delta(p-a)]$. The resulting mode is an antisymmetric function

$$\psi = N \begin{cases} -U_0 a^2 - (U_0 a - 1)p & p < -a \\ p & |p| \leq a \\ U_0 a^2 - (U_0 a - 1)p & p > a, \end{cases} \quad (7)$$

where N is a normalization constant. For the values $U_0 \approx 7.73$ and $a \approx 0.445$ listed above, the mode vanishes at $p_c \approx \pm 0.627$ which corresponds to $0.534 \leq r \leq 1.872$. This is a remarkably good result given the simplicity of this type of approximation, which is used in many areas of quantum mechanics [29]. Similarly, for a single-well potential (appropriate to the catenoid [15]), by replacing $2\text{sech}^2 p$ with $2\delta(p)$ the resulting mode consists of a symmetric triangular function with the correct linear asymptotic growth as $x \rightarrow \pm\infty$. The critical value p_c that determines stability of the shape is $p_c = 1$, instead of the exact value $p_c = 1.2$, which, though not as accurate as for the double well, is still not a bad approximation.

An alternative approach to the determination of p_c is to view the term $-2KW$ in the Jacobi equation as a perturbation ϵV to the Dirichlet eigenvalue equation $(\nabla^2 + \epsilon V)\psi = \lambda\psi$ for a flat rectangular membrane. Writing $\psi = \psi_0 + \epsilon\psi_1 + \dots$ and $\lambda = \lambda_0 + \epsilon\lambda_1 + \dots$, one finds the standard perturbation theory result $\lambda_1 = \frac{\int \int d\theta dp V \psi_0^2}{\int \int d\theta dp \psi_0^2}$. Then, using the lowest eigenfunction consistent with the boundary conditions, $\psi_0 \sim \cos\theta \cos(\pi p/2p_0)$, the critical value p_c is that which makes the first-order-corrected eigenvalue equal to zero. We obtain, numerically, the condition $p_c \approx 0.536$ ($r_c \approx 0.585$), in good agreement with the results above.

We now turn to the systolic curve on a Meeks Möbius surface. In the absence of analytical results on the shape of such a geodesic, we employ a numerical scheme introduced recently [18]. This method is based on the use of the curve length L as a Lyapunov function in a gradient flow relaxational scheme. In (r, θ) coordinates,

$$L = \int_0^{2\pi} d\theta \left[E \left(\frac{dr}{d\theta} \right)^2 + G \right]^{1/2}, \quad (8)$$

where $E = \mathbf{X}_r \cdot \mathbf{X}_r$, and $G = \mathbf{X}_\theta \cdot \mathbf{X}_\theta$. If we define $g = Er_\theta^2 + G$, then we use a local Rayleigh dissipation function [30] to obtain, $r_t = -(1/\sqrt{g})\delta L/\delta r$, which is the nonlinear diffusion equation

$$\frac{\partial r}{\partial t} = \frac{1}{\sqrt{g}} \frac{\partial}{\partial \theta} \left(\frac{E}{\sqrt{g}} \frac{\partial r}{\partial \theta} \right) - \frac{1}{2g} \left[E_r \left(\frac{\partial r}{\partial \theta} \right)^2 + G_r \right]. \quad (9)$$

This is a version of the curve-shortening equation [31] on a curved manifold [32]. Our goal is to find the function $r(\theta)$ for which the rhs of (9) vanishes. Since the Meeks surface contains the circle $r = 1$, this may be taken as a suitable initial condition for the dynamics. This curve naturally has a linking number of 1 with respect to the boundary curve, a property that is maintained throughout the evolution.

The numerically obtained systolic curve \mathcal{C}_M for the critical Meeks surface is shown in Fig. 3(a), superimposed on the surface. As in other examples studied to date [18], much of this systolic curve lies on the catenoidlike neck of the surface. Figure 3(b) shows, on a contour plot of the unstable eigenfunction ψ_c , that \mathcal{C}_M passes very near the maximum of the unstable mode. An approximate analytical form for the systole is $\cos\theta = -(1/2)\sinh p - \cosh p \tanh 2p$, which coincides with the result of extremizing the denominator in Eq. (4) with respect to p only. This approximation shares with the full numerical result the feature of tracking the ridge in the Gaussian curvature and passes near the maximum of the marginal eigenfunction. Previously [18], we conjectured that if the local systolic curve \mathcal{C} is linked to the boundary $\partial\mathcal{S}$, then the singularity that occurs when the minimal surface becomes unstable will be on $\partial\mathcal{S}$, otherwise, it will be in the bulk. The present results lead to the additional

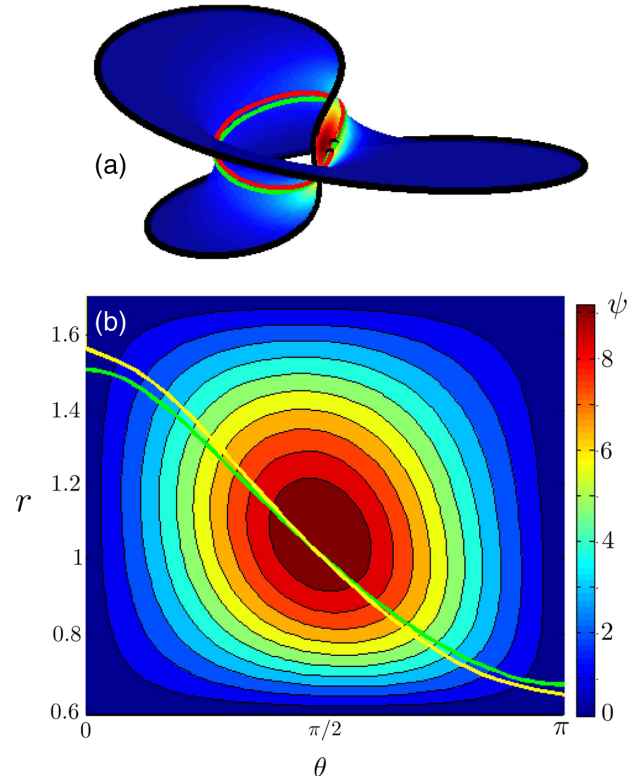


FIG. 3 (color online). Properties of the systolic curve. (a) The critical Meeks Möbius surface with the numerically obtained systolic curve (green), and approximation (red). (b) Systolic curve (green) and approximation (yellow) traced out in the (r, θ) plane, superimposed over the unstable mode.

conjecture that, when a neck on a minimal surface \mathcal{S} becomes unstable, the local systolic curve \mathcal{C} passes through the neighborhood of the maximum of the unstable mode.

In the same way that the catenoid serves as a paradigm for the study of bulk singularities that follow from instabilities of an orientable minimal surface, the results presented here suggest that the truncated Meeks Möbius strip is the counterpart for the study of boundary singularities occurring in nonorientable surfaces. Furthermore, the correspondence between systolic curves, the critical points of the curvature potential $-2KW$, and the structure of the unstable eigenfunction is reminiscent of Witten's formulation of Morse theory [33] and suggests an avenue for future analysis.

We are grateful to P. Constantin, P. Figueras, M. Gromov, L. Guth, R. Kusner, and W. Meeks for discussions, and thank A. Iserles and M. J. Shelley for advice on numerical methods. This work was supported in part by EPSRC Grant No. EP/IO36060/1 and the Schlumberger Chair Fund.

-
- [1] M. Berger, What is ... a Systole? *Not. Am. Math. Soc.* **55**, 374 (2008).
- [2] L. Euler, Curvarum maximi minimive proprietate gaudentium inventio nova et facilis, *Commentarii Academiae Scientiarum Imperialis Petropolitanae* **8**, 159 (1741).
- [3] C. Isenberg, *The Science of Soap Films and Soap Bubbles* (Dover, New York, 1992).
- [4] P. Zihler and R. D. Kamien, Soap Froths and Crystal Structures, *Phys. Rev. Lett.* **85**, 3528 (2000).
- [5] R. D. Kamien and T. C. Lubensky, Minimal Surfaces, Screw Dislocations, and Twist Grain Boundaries, *Phys. Rev. Lett.* **82**, 2892 (1999).
- [6] D. Christodoulou, *Mathematical Problems of General Relativity I* (European Mathematical Society, Zurich, 2000).
- [7] J. M. Maldacena, Wilson Loops in Large N Field Theories, *Phys. Rev. Lett.* **80**, 4859 (1998); N. Drukker, D. J. Gross, and H. Ooguri, Wilson Loops and Minimal Surfaces, *Phys. Rev. D* **60**, 125006 (1999).
- [8] M. Emmer, Minimal Surfaces and Architecture: New Forms, *Nexus Netw. J.* **15**, 227 (2013).
- [9] J. B. Bostwick and P. H. Steen, Stability of Constrained Capillary Surfaces, *Annu. Rev. Fluid Mech.* **47**, 539 (2015).
- [10] C. W. B. Goldschmidt, Determinatio Superficie Minima Rotatione Curvae Data Duo Puncta Jungentis Circa Datum Axem Artae PhD thesis, Göttingen, 1831.
- [11] S. A. Cryer and P. H. Steen, Collapse of a soap-film bridge: quasistatic description, *J. Colloid Interface Sci.* **154**, 276 (1992); Y. J. Chen and P. H. Steen, Dynamics of inviscid capillary breakup: collapse and pinch-off of a film bridge, *J. Fluid Mech.* **341**, 245 (1997); N. D. Robinson and P. H. Steen, Observations of Singularity Formation during the Capillary Collapse and Bubble Pinch-off of a Soap Film Bridge, *J. Colloid Interface Sci.* **241**, 448 (2001); M. Nitsche and P. H. Steen, Numerical simulations of inviscid capillary pinch-off, *J. Comput. Phys.* **200**, 299 (2004).
- [12] D. Leppinen and J. R. Lister, Capillary pinch-off in inviscid fluids, *Phys. Fluids* **15**, 568 (2003).
- [13] L. Lehner and F. Pretorius, Black Strings, Low Viscosity Fluids, and Violation of Cosmic Censorship, *Phys. Rev. Lett.* **105**, 101102 (2010).
- [14] J. C. C. Nitsche, *Lectures on Minimal Surfaces* (Cambridge University Press, Cambridge, England, 1989), Vol. I.
- [15] A. Boudaoud, P. Patricio, and M. Ben Amar, The Helicoid versus the Catenoid: Geometrically Induced Bifurcations, *Phys. Rev. Lett.* **83**, 3836 (1999).
- [16] R. E. Goldstein, H. K. Moffatt, A. I. Pesci, and R. L. Ricca, Soap-film Möbius strip changes topology with a twist singularity, *Proc. Natl. Acad. Sci. U.S.A.* **107**, 21979 (2010).
- [17] R. E. Goldstein, H. K. Moffatt, and A. I. Pesci, Topological constraints and their breakdown in dynamical evolution, *Nonlinearity* **25**, R85 (2012).
- [18] R. E. Goldstein, J. McTavish, H. K. Moffatt, and A. I. Pesci, Boundary singularities produced by the motion of soap films, *Proc. Natl. Acad. Sci. U.S.A.* **111**, 8339 (2014).
- [19] M. Katz, *Systolic Geometry and Topology*, Mathematical Surveys and Monographs, Vol. 137 (American Mathematical Society, Providence, RI, 2007).
- [20] For a summary of open problems in systolic geometry, see <http://u.cs.biu.ac.il/~katzmik/sgt.html>.
- [21] M. H. Freedman, D. A. Meyer, and F. Luo, in *Mathematics of Quantum Computation*, Computational Mathematics Series (Chapman & Hall/CRC, Boca Raton, FL, 2002), pp. 287–320.
- [22] W. H. Meeks, III, The classification of complete minimal surfaces in \mathbf{R}^3 with total curvature greater than -8π , *Duke Math. J.* **48**, 523 (1981).
- [23] J. Oprea, *Differential Geometry and Its Applications* (The Mathematical Association of America, Washington, DC, 2007); W. H. Meeks, III, and J. Pérez, *A Survey on Classical Minimal Surface Theory* (American Mathematical Society, Providence, RI, 2012).
- [24] M. do Carmo and C. K. Peng, Stable complete minimal surfaces in \mathbf{R}^3 are planes, *Bull. Am. Math. Soc.* **1**, 903 (1979).
- [25] M. Ross, Complete nonorientable minimal surfaces in \mathbf{R}^3 , *Commentarii mathematici Helvetici* **67**, 64 (1992).
- [26] N. Rosen and P. Morse, On vibrations of polyatomic molecules, *Phys. Rev.* **42**, 210 (1932).
- [27] B. Stec, Solution of a one-dimensional Schrödinger equation for a double-well potential with finite walls, *Acta Phys. Pol. A* **68**, 681 (1985).
- [28] *Heun's Differential Equations*, edited by A. Ronveaux (The Clarendon Press, Oxford, 1995).
- [29] For a recent example in the context of Bose-Einstein condensation, see H. Cartarius and G. Wunner, Model of a \mathcal{PT} -symmetric Bose-Einstein condensate in a δ -function double-well potential, *Phys. Rev. A* **86**, 013612 (2012).
- [30] S. A. Langer, R. E. Goldstein, and D. P. Jackson, Dynamics of labyrinthine pattern formation in magnetic fluids, *Phys. Rev. A* **46**, 4894 (1992).
- [31] M. Gage and R. S. Hamilton, The heat equation shrinking convex plane curves, *J. Diff. Geom.* **23**, 69 (1986).
- [32] M. A. Grayson, The heat equation shrinks embedded plane curves to round points, *J. Diff. Geom.* **26**, 285 (1987).
- [33] E. Witten, Supersymmetry and Morse theory, *J. Diff. Geom.* **17**, 661 (1982).